

Electroreduction of Organic Compounds, 35 [1]. Quantum Chemical Calculations of Reaction Pathways for the Cathodic Dehalogenation of Chlorodibenzofurans and Oligochlorobenzenes

Dirk Golinske and Jürgen Voss

Institut für Organische Chemie der Universität Hamburg, Martin-Luther-King-Platz 6,
D-20146 Hamburg, Germany

Reprint requests to Prof. Dr. Jürgen Voss. Fax: +49 (0) 40 42838 5592.
E-mail: voss@chemie.uni-hamburg.de.

Z. Naturforsch. **60b**, 780–786 (2005); received October 18, 2004

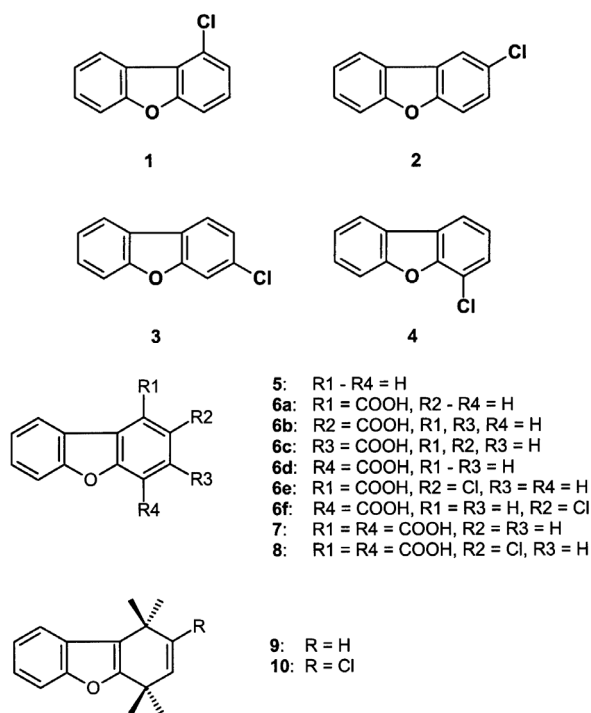
Quantum chemical (DFT) calculations on the course of the electroreductive carboxylation of chloroarenes were performed. An explanation for the extraordinary behaviour of 2-chlorodibenzofuran (**2**) as compared with the corresponding 1-chloro, 3-chloro and 4-chloro derivatives was sought for and was found in the particular reaction coordinate of **2** and in the SOMO spin density distributions of the four isomers. In the same way, the regioselectivity in the formation of dicarboxylic acids from hexachloro- and 1,2,4,5-tetrachlorobenzene was investigated by DFT-MO calculations and was shown to be due to orbital effects besides steric hindrance.

Key words: Cathodic Dehalogenation, Reaction Mechanism, DFT-MO Calculations

Introduction

The four regioisomers of monochlorodibenzofuran (**1–4**) exhibit significant differences in reactivity and product selectivity during the electroreductive dehalogenation [2, 3].

In particular, 2-dichlorodibenzofuran (**2**) represents a special case. Its electrochemical reduction (hydrodechlorination) and carboxylation is considerably impeded as compared with the other three isomers and, moreover, it forms completely unexpected products. Whereas 1-chloro- (**1**), 3-chloro- (**3**) and 4-chlorodibenzofuran (**4**) yield dibenzofuran (**5**) and 1,4-dihydrodibenzofuran (**9**) by electrolysis in methanol, 2-chlorodibenzofuran (**2**) gives 2-chloro-1,4-dihydrodibenzofuran (**10**) as the main product (56% yield) [4, 5]. The electrocarboxylation of **1**, **3** and **4** expectedly results in the formation of the corresponding carboxylic acids **6a**, **6c** and **6d** as the main products together with minor amounts of hydrogenated compounds. However, not even traces of dibenzofuran-2-carboxylic acid (**6b**) are produced from **2**. Instead, a complicated mixture of different carboxylic acids is formed with dibenzofuran-1,4-dicarboxylic acid (**7**) (30% yield) and 2-chlorodibenzofuran-1,4-dicarboxylic acid (**8**) (20% yield) as the main products



and 11% of a mixture of further carboxylic acids which also retain a chloro substituent in the 2-position [2, 3].

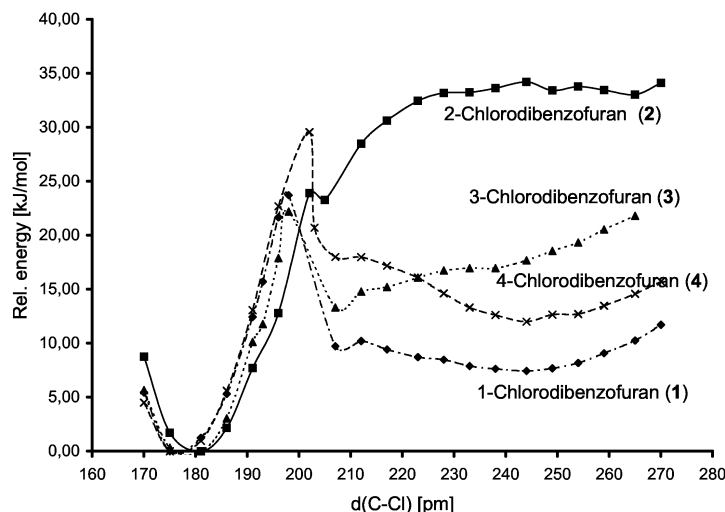


Fig. 1. Reaction coordinates for the electroreductive dehalogenation of the chlorodibenzofurans ($\diamond = 1$, $\blacksquare = 2$, $\blacktriangle = 3$, $\times = 4$) as calculated by the DFT method.

In order to explain this strange behaviour of **2** we have performed MO calculations of the reaction paths and the spin density distribution in **1–4**. The aim of our calculations was to find the particular step of the reaction cascade in which the differences in reactivity occur.

Results and Discussion

In principle, the electrochemical dehalogenation of chloroarenes [6] takes place in four steps [7]. First an electron is transferred to the substrate molecule at the cathode. The radical anion $\text{Ar-X}^{\bullet-}$ thus formed eliminates a chloride anion to yield the radical Ar^{\bullet} . This takes up another electron at the cathode (ECEC mechanism) or, alternatively, by disproportionation (DISP mechanism). The resulting carbanion Ar^- finally reacts with an electrophile E^+ present such as a proton or carbon dioxide in the case of electrocarboxylation.

ECEC mechanism:	DISP mechanism:
(1) $\text{Ar-X} + \text{e}^- \rightleftharpoons \text{Ar-X}^{\bullet-}$	(1) $\text{Ar-X} + \text{e}^- \rightleftharpoons \text{Ar-X}^{\bullet-}$
(2) $\text{Ar-X}^{\bullet-} \rightarrow \text{Ar}^{\bullet} + \text{X}^-$	(2) $\text{Ar-X}^{\bullet-} \rightarrow \text{Ar}^{\bullet} + \text{X}^-$
(3) $\text{Ar}^{\bullet} + \text{e}^- \rightarrow \text{Ar}^-$	(3) $\text{Ar}^{\bullet} + \text{Ar-X}^{\bullet-} \rightarrow \text{Ar}^- + \text{Ar-X}$
(4) $\text{Ar}^- + \text{E}^+ \rightarrow \text{Ar-E}$	(4) $\text{Ar}^- + \text{E}^+ \rightarrow \text{Ar-E}$

The experimental evidence suggests the primary radical anion $\text{Ar-X}^{\bullet-}$ to be the most important species in the reaction sequence. The deciding contribution to the activation energy of the overall reaction is possibly given by the heterogeneous electron transfer at the electrode [step (1)]. This can, however, in any case be easily achieved by a proper choice of the reduction potential. The real differences in reactivity and selectiv-

ity become apparent in the follow-up reactions of the radical anions $\text{Ar-X}^{\bullet-}$ in the bulk of the solution. In particular, the chloride anion elimination from these radical anions should play a deciding role. We concentrated our quantum chemical calculations therefore on the electronic structure of $\text{Ar-X}^{\bullet-}$ and on step (2) of the reaction sequence. The calculations were performed by use of the density functional (DFT) pBP method [8]. The required starting geometries of the radical anions were pre-optimised with the force field method SYBYL implemented in the software SPARTAN which we applied. The charge was set at -1 (doublet state of the radical anion) and the DN* basis set was used for the DFT calculations. The length of the C-Cl bond in the radical anion was elongated in steps of 5 pm from 170 pm to 270 pm for the calculation of the reaction path. The geometry of the radical anion including the out-of-plane angle of the chloro substituent was optimised for each step. – Solvation of the reacting species was not considered in our calculations although it plays an important role. Especially, free chloride ions do not occur in the solution but are stabilised by ion pairing and interactions with the solvent molecules [9].

The relevant section of the reaction coordinate is obtained as the graph of the calculated molecular energies of each step versus the C-Cl distances. Fig. 1 shows the reaction coordinates which result from DFT calculations.

Obviously the chloride elimination from the radical anion of 2-chlorodibenzofuran (**2**) would take place without any gain of energy in contrast to the elimi-

nation of the 1-chloro- (**1**), the 3-chloro- (**3**) and the 4-chlorodibenzofuran (**4**) radical anions, which exhibit more or less pronounced energy minima in the reaction pathway.

The transition state geometries for the chloride elimination of **1**^{•−}–**4**^{•−} are shown in Fig. 2. One can recognize that, in the case of **1**, **3** and **4**, an out-of-plane bending of the C-Cl bond [10] occurs. The local minima are assigned to the radical anions and one can make out the following order for the bond breaking steps. The dissociation of the radical anion of **2** occurs at the latest (at a C-Cl distance of 203 pm) whereas the other radical anions lose the chloride anion at 201 pm (**4**), at 198 pm (**1**) and at 196 pm (**3**). The earlier the C-Cl bond is cleaved the easier the corresponding monochlorodibenzofuran should be dechlorinated by electroreduction. This result is in agreement with the experimental irreversible reduction potentials, which increase in the order [11]

$$E_{\text{red}}(\mathbf{4}) = -2.03 \text{ V} < E_{\text{red}}(\mathbf{1}) = -2.05 \text{ V} \\ < E_{\text{red}}(\mathbf{3}) = -2.06 \text{ V} \ll E_{\text{red}}(\mathbf{2}) = -2.18 \text{ V}.$$

The bending of the C-Cl bonds in **1**^{•−}, **3**^{•−} and **4**^{•−} can be understood as a re-hybridisation which transforms the planar π -radical anion into a kind of σ -radical with side-on coordination. This would also facilitate the attack of an electrophile such as carbon dioxide or a proton from the backside of the arene ring before even the chloro substituent is completely removed. On the other hand, **2**^{•−} remains planar ($\delta = 177^\circ$) and, as a consequence, is more resistant to substitution of the chloro substituent.

Besides the energy profiles of the reactions the spin densities in the SOMOs of the radical anions should provide important information about the differences in the reactivity and, in particular, the selectivity of **1**–**4** during the electroreduction. The cleavage of the C-Cl bond should be the easier the higher the spin density (charge density) at the carbon centre with the chloro substituent is because this would destabilize the C-Cl bond. Beland *et al.* have, for instance, shown that electron density distributions as calculated by semi-empirical MO calculations allow reasonable predictions of the product distributions observed for the electroreduction of chlorobenzene congeners [12]. Our DFT type MO calculations clearly show that **1**, **3** and **4** exhibit considerable SOMO spin densities in the 1-, the 3-, and the 4-position, respectively, whereas the spin density in the 2-posi-

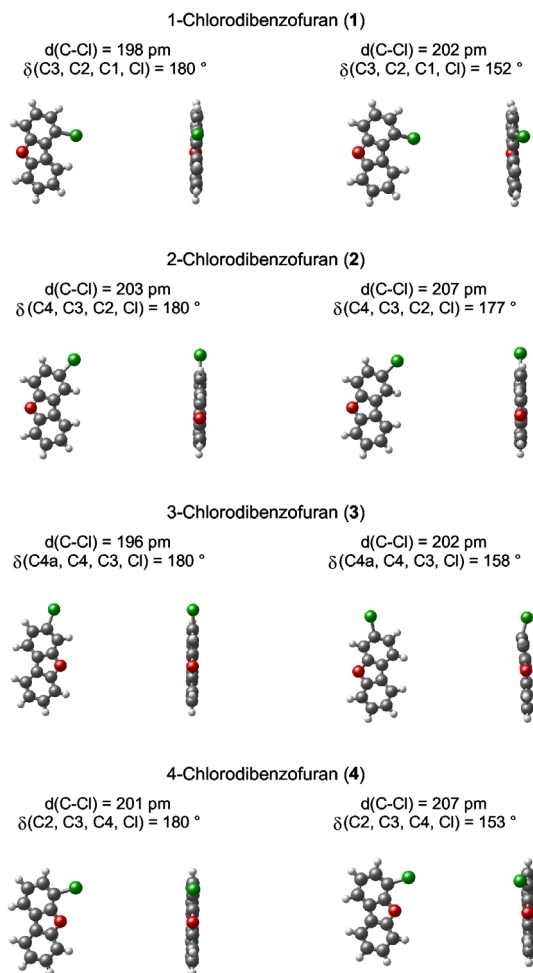


Fig. 2. Distances $d(\text{C-Cl})$ and out-of-plane bending angles δ in the chlorodibenzofuran radical anions **1**^{•−}–**4**^{•−}; a) at the transition state for the electroreductive dechlorination (left) and b) after further elongation of the C-Cl bond (right).

tion of **2** (as well as of **1**, **3**, **4** and **5**) is virtually zero (Fig. 3).

Therefore, a displacement of the chloro substituent does not occur in **2**. Instead, other reactions such as attack of protons or carbon dioxide at the 1- and the 4-position take place to yield the observed products.

The question which then arose was how the spin density distribution in the SOMOs would depend on the C-Cl distance. To answer this question we have calculated the spin densities of the exemplary radical anions **2**^{•−} and **3**^{•−} at the deciding points of the reaction coordinate. The results are shown in Fig. 4.

One can see, that the chloride anion draws over the electron density while it is leaving the molecule. The

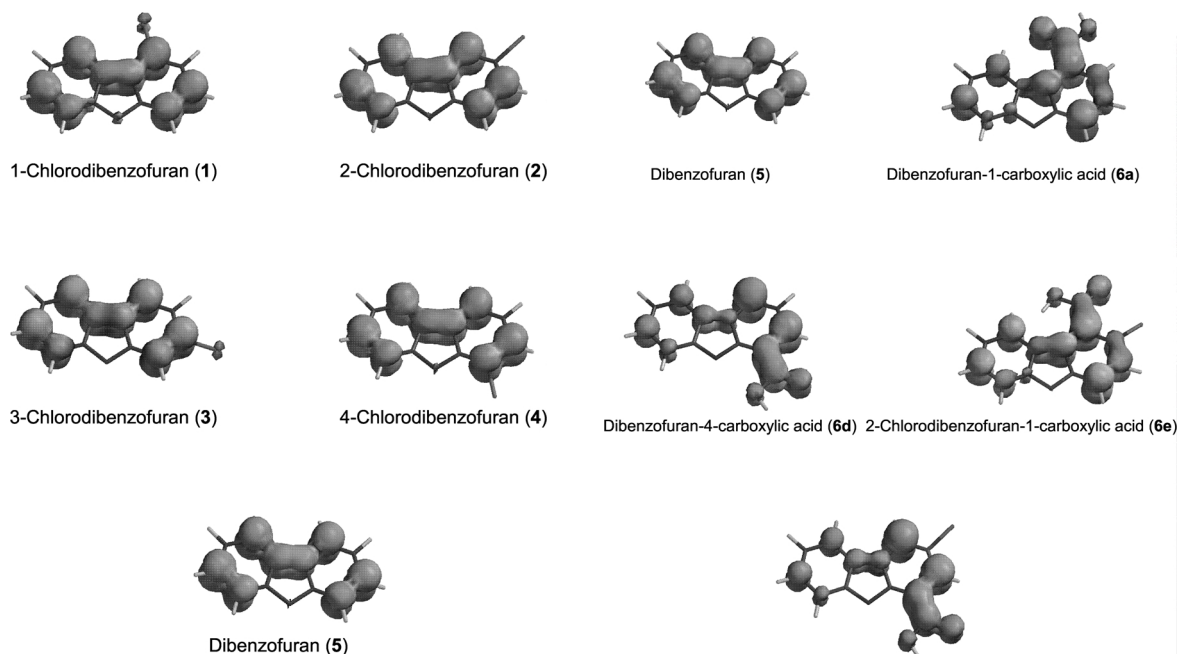


Fig. 3. Spin density distribution in the SOMOs of the chlorodibenzofuran radical anions $1^{\bullet-}$ – $5^{\bullet-}$.

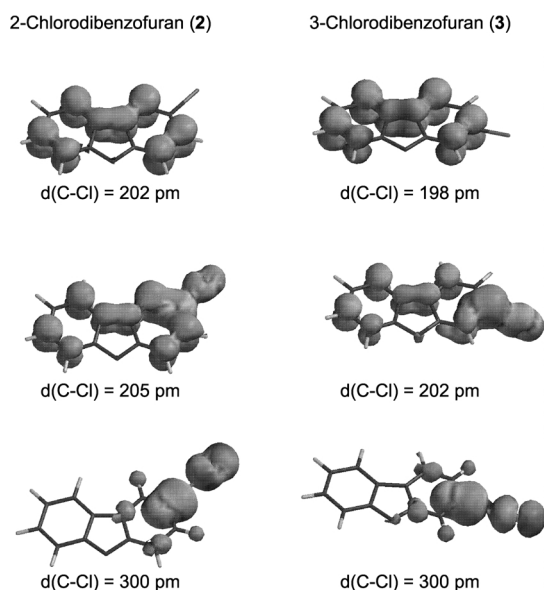


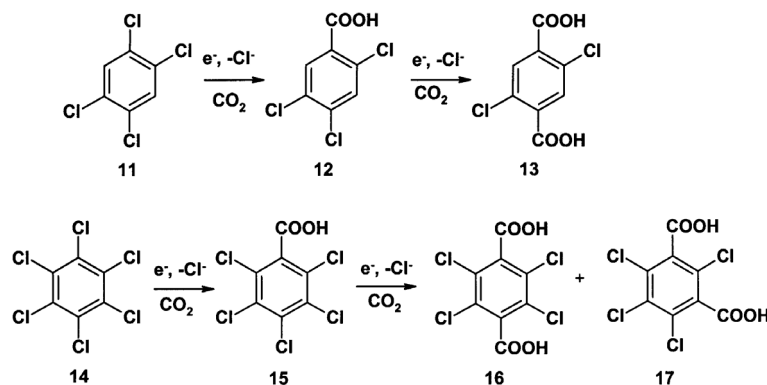
Fig. 4. Spin density distribution in the SOMOs of $2^{\bullet-}$ (left) and $3^{\bullet-}$ (right) at different C-Cl distances as calculated by the DFT method.

π -type SOMO is thereby transformed into an antibonding σ^* -SOMO. These calculations once more clearly demonstrate that 2-chlorodibenzofuran (2) behaves exceptional during the reductive dechlorination.

Fig. 5. Spin density distribution in the SOMOs of $5^{\bullet-}$, $6a^{\bullet-}$, $6d^{\bullet-}$, $6e^{\bullet-}$ and $6f^{\bullet-}$ as calculated by the DFT method.

In order to understand the particular reactivity at the 1- and the 4-position with respect to displacement reactions we have also calculated the SOMO spin density distributions in dibenzofuran (5), in dibenzofuran-1- (6a) and in dibenzofuran-4-carboxylic acid (6d) (Fig. 5).

Whereas 5 itself and its monochloro derivatives 1–4 (Fig. 3) exhibit almost identical SOMOs the spin densities of 6a and 6d considerably deviate from the former. Obviously the spin densities at the 4-position of 6a and at the 1-position of 6d are higher as compared with all other positions of the ring system including the respective 2- and 3-positions. This result very well explains the experimental observation that during electroreduction the second attack of an electrophile occurs at the 1- and at the 4-position. Therefore, dibenzofuran-1,4-dicarboxylic acid (7) is formed as product of the electrocarboxylation of 1–4 and also of 5. The latter most probably is transformed stepwise into 7 via the monocarboxylic acids 6a and/or 6d, which are indeed found as by-products after electrocarboxylation of 5 itself. — Similarly, the electrocarboxylation of 2 to form 8 as a major product should occur by first attack at the 1- and subsequently at the activated 4-position or vice versa. The deactivated 2-position in the presumable in-



intermediates 2-chlorodibenzofuran-1-carboxylic (**6e**) or 2-chlorodibenzofuran-4-carboxylic acid (**6f**) remains untouched during the reaction sequence since the spin densities are virtually zero in that position (see Fig. 5).

1,2,4,5-Tetrachloro- and hexachlorobenzene

Benzenes with up to three chloro substituents are transformed into the corresponding benzene monocarboxylic acids during electroreduction in the presence of carbon dioxide [13]. However, 1,2,4,5-tetrachlorobenzene (**11**) yields 17% of 2,5-dichlorobenzene-1,4-dicarboxylic acid (**13**) among other products, and hexachlorobenzene (**14**) yields 10% of tetrachlorobenzene-1,4-dicarboxylic acid (**16**) plus 8% of tetrachlorobenzene-1,3-dicarboxylic acid (**17**) besides 64% of the main product pentachlorobenzoic acid (**15**) [2]. The observation of these restricted but nevertheless regioselective electrocarboxylation reactions raised the question whether the introduction of a carboxy substituent into the arene molecule deactivates the electrochemical dechlorination. We have therefore performed DFT calculations on the reaction pathways for the electrocarboxylation of **14** and of the spin density distribution in **11** and **14**.

The reaction coordinates for the elimination of chloride from the 2-, 3- and 4-position of pentachlorobenzoic acid (**15**) are shown in Fig. 6.

No local energy maximum for the elimination is found in any of the three reaction pathways. Thus the reactions are devoid of activation. Interestingly however, the global energy minimum for the elongation of the C-4-Cl bond is significantly shifted to a longer distance of 191 pm as compared with ca. 180 pm for the C-2-Cl bond and the C-3-Cl bond. This effect may be the reason for the observed substitution in the 4-position, *i. e.* the preferred formation of **16** from **15**.

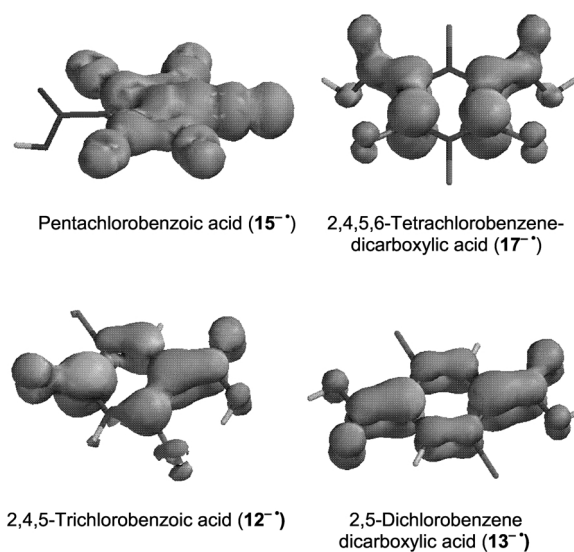


Fig. 6. Reaction coordinates for the chloride elimination from the 2-, 3- and 4-position of the pentachlorobenzoic acid radical anion **15**^{•-} as calculated by the DFT method.

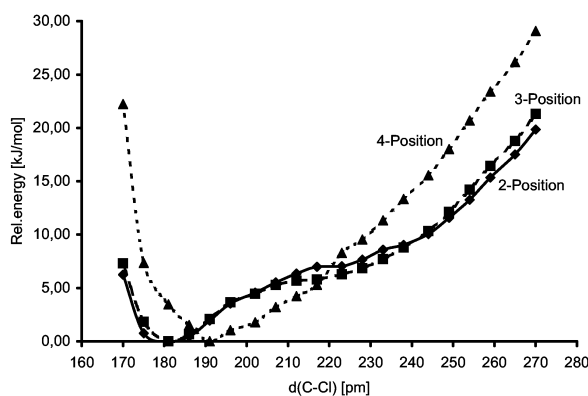


Fig. 7. Spin density distribution in the SOMOs of **15**^{•-}, **17**^{•-}, **12**^{•-} and **13**^{•-}.

If furthermore the spin density distribution in the radical anion of **15** is taken into consideration (Fig. 7) the C-4-Cl bond turns out to exhibit the highest SOMO spin density and should therefore be the weakest one.

These results agree well with the experimental facts, *i.e.* the formation of only minor amounts of dicarboxylic acids, mainly **16** and even less **17**, as by-products [2]. A further carboxylation step of **16** to form a tricarboxylic acid is completely unlikely on account of the steric hindrance in the *ortho*-positions. The SOMO spin density in the radical anion of **17** (Fig. 7) clearly shows that only the 4(6-)-position is electronically suitable for the attack of an electrophile. This position exhibits, however, the same steric hindrance as the *ortho*-positions in **16**.

A similar situation is found for the electrocarboxylation of 1,2,4,5-tetrachlorobenzene (**11**). The two major products which are formed, 2,4,5-trichlorobenzoic acid (**12**) and 2,5-dichlorobenzene-1,4-dicarboxylic acid (**13**), are in accordance with the pattern of substituents in **15** and **16** formed from **14**. Thus, the same regioselectivity is observed [2]. The spin density distribution in the SOMO of the 2,4,5-trichlorobenzoic acid radical anion (**12**^{•-}) is high in the 1- and in the 4-position (Fig. 7). The C-4-Cl bond should be weakened because an antibonding σ^* -SOMO is being created. Substitution will therefore occur in the 4-position and as the result **13** is obtained. Further follow-up reactions of **13** are prohibited by steric hindrance and also by the unfavourable spin density distribution in the SOMO of **13**^{•-} (Fig. 7). Only the *ipso*-positions (C1 and C4) exhibit high spin densities whereas the C-Cl bonds do not. Even a hydrodechlorination of **13**, *i.e.* the displacement of a chloro substituent by a proton is not observed which cannot underlie to steric hindrance but must be due to the unfavourable spin density distribution.

Conclusion

The extraordinary stability of the C-2-Cl bond in 2-chlorodibenzofuran (**2**) which strongly inhibits the displacement of the chloro substituent by electroreduction is explained in terms of the very low SOMO spin density in the 2-position of dibenzofurans as calculated by the DFT method. As a consequence of this fact no significant energy minimum is found in the corresponding reaction coordinate of **2** in contrast to the case of the other three isomers.

Similarly, the specific behaviour of 2,4,5-trichlorobenzoic acid (**12**) and pentachlorobenzoic acid (**15**) is shown to be due to high spin densities in the 4-position which loosens the C-4-Cl bond and directs the second chloride displacement by carbon dioxide into this position.

Calculations

The MO calculations were carried out by use of a Silicon Graphics computer "OCTANE" (R 10000) and a Siemens Nixdorf parallel computer SC 900 (18 Mips R 10000).— The software package SPARTAN 5.1 of Wavefunction Inc. [14, 15] was used. — The geometries of the molecules were pre-optimised by molecular mechanics calculations using the SYBYL program which is implemented in the SPARTAN software. The DFT-based geometry optimisations and spin density calculations were performed by the B3LYP/6-31G* method [8].

Acknowledgements

Support of this work by the "Universität Hamburg", the "Deutsche Forschungsgemeinschaft" (SFB 188) and the "Bundesministerium für Bildung und Forschung" (BMBF, FK7 0318896C) is gratefully acknowledged.

- [1] Part 34: O. Kranz, J. Voss, Z. Naturforsch. **58b**, 1187 (2003).
- [2] D. Golinske, J. Voss, G. Adiwidjaja, Collect. Czech. Chem. Commun. **65**, 862 (2000).
- [3] D. Golinske, Elektrochemische Enthalogenieierung halogenierter Aromaten in Gegenwart verschiedener Elektrophile, Dissertation, Universität Hamburg (2002). — "der andere verlag", Osnabrück (2002), ISBN 3-936231-25-7.
- [4] M. Altrogge, Elektrochemische Enthalogenieierung chlorierter Biphenyle, Dibenzofurane und Dibenzo-p-dioxine, Dissertation, Universität Hamburg (1992). —

- J. Voss, M. Altrogge, H. Wilkes, W. Francke, Z. Naturforsch. **46b**, 400 (1991).
- [5] E. Waller, Elektrochemische Enthalogenieierung polychlorierter Naphthaline sowie Elektroreduktion monochlorierter Dibenzofurane, Dissertation, Universität Hamburg (1997). — Shaker Verlag, Aachen (1998), ISBN 3-8265-3500-6. J. Voss, E. Waller, P. Kränke, J. Prakt. Chem. **340**, 430 (1998).
- [6] Aliphatic chlorocompounds do not form stabilised radical anions. They are dechlorinated by a concerted electron uptake with simultaneous chloride elimination. — L. Salem, Electrons in Chemical Reactions:

- First Principles, chapt. 5, Wiley, New York (1982).
B. Bigot, D. Roux, L. Salem, J. Am. Chem. Soc. **103**, 5271 (1981). C. P. Andrieux, A. L. Gorande, J.-M. Savéant, J. Am. Chem. Soc. **114**, 6892 (1992); see also ref. [7].
- [7] M. Borsari, C. Fontanesi, G. Gavioli, Curr. Top. Electrochem. **5**, 167 (1997) and lit. cited therein.
- [8] A. D. Becke, Phys. Rev. A **33**, 3098 (1988).
- [9] E. Canadell, P. Karafiloglou, L. Salem, J. Am. Chem. Soc. **102**, 855 (1980).
- [10] Similar deformations of the transition states have also been found for the electroreduction of chloroanisoles [O. Kranz, Elektroreduktion chlorierter Aromaten und Dipropylether in protischen Lösungsmitteln, Dissertation, Universität Hamburg (2000)] and of 4-chlorotoluene [C. Fontanesi, J. Mol. Struct. (Theochem) **392**, 87 (1997)].
- [11] As measured vs. an internal Ag/AgBr reference electrode in MeOH, see ref. [4, 5].
- [12] F. A. Beland, S. O. Farwell, P. R. Callis, R. D. Geer, J. Electroanal. Chem. **78**, 145 (1977).
- [13] J. Chaussard, J.-C. Folest, J.-Y. Nédélec, J. Périchon, S. Sibille, M. Troupel, Synthesis 369 (1990) and lit. cited therein.
- [14] W. J. Hehre, J. Yu, P. H. Kluzinger, A Guide to Molecular Mechanics and Molecular Orbital Calculations in SPARTAN, Wavefunction Inc., Irvine CA (1997).
- [15] W. J. Hehre, L. Lou, A Guide to Density Functional Calculations in SPARTAN, Wavefunction Inc., Irvine CA (1997).